

## Local zooming genetic algorithm and its application to radial gate support problems

Young-Doo Kwon<sup>†</sup>

*School of Mechanical Engineering, Kyungpook National University, Daegu 702-701, Korea*

Seung-Bo Jin<sup>‡</sup>

*System Design & Integration Department, KSLV Systems Division,  
Korea Aerospace Research Institute, Korea*

Jae-Yong Kim<sup>‡</sup>

*Korea Atomic Energy Research Institute, Korea*

Il-Hee Lee<sup>‡†</sup>

*Voith Turbo, Co., Korea*

*(Received January 9, 2003, Accepted October 9, 2003)*

**Abstract.** On the basis of a structural analysis of radial gate (i.e. Tainter gate), the current paper focuses on weight minimization according to the location of the arms on a radial gate. In spite of its economical significance, there are hardly any previous studies on the optimum design of radial gate. Accordingly, the present study identifies the optimum position of the support point for a radial gate that guarantees the minimum weight satisfying the strength constraint conditions. This study also identifies the optimum position for 2 or 3 radial arms with a convex cylindrical skin plate relative to a given radius of the skin plate curvature, pivot point, water depth, ice pressure, etc. These optimum designs are then compared with previously constructed radial gates. Local genetic and hybrid-type genetic algorithms are used as the optimum tools to reduce the computing time and enhance the accuracy. The results indicate that the weights of the optimized radial gates are appreciably lower than those of previously constructed gates.

**Key words:** DFP method (Davidon-Fletcher-Powell Method); genetic algorithm hybrid method; LZGA (Local Zooming Genetic Algorithm); radial gate (Tainter gate); 2-arm type; 3-arm type.

---

<sup>†</sup> Professor  
<sup>‡</sup> Researcher  
<sup>‡†</sup> Director

## 1. Introduction

The optimum techniques are categorized into two groups. One is the local search (gradient method) group. The steepest descent method is very powerful in simple cases. However, the convergence rate may be too slow in some problems, like a curved sharp valley. The DFP method is a kind of the variable metric algorithm, which can solve that kind of problem without any difficulty. It uses conjugate directions, if the objective function is quadratic (Himmelblau 1972). The traditional gradient method only focuses on searching the local extremum near the current points.

In contrast, the other is the global search group. The genetic algorithms are stochastic global search methods based on the mechanism of natural selection and natural genetics. Therefore, GA (genetic algorithm) have recently been applied to structural optimization problems due to their capability of solving optimum problems that involve mixing continuous, discontinuous, and non-convex regions etc. The SGA (simple GA) is improved to MGA (micro GA) by using some techniques like tournament selection along with the elitist strategy. Yet, the GA has more difficulty in fast searching the exact optimum point at later stage. The DPE (Dynamic Parameter Encoding) GA (Schraudolph 1992) uses a digital zooming technique, which means that the digit of higher rank is not changed any more after a certain stage. The SZGA (Successive Zooming GA) zooms the searching area successively, thus the convergence rate is highly increased (Kwon 2003). The SZGA might lose the optimum point, if the zooming factor is not properly chosen. Therefore, we propose a new GA technique, which guarantee to find the optimum point. The remaining global search techniques are SA (Simulated Annealing) and PGSL (Probabilistic Global Search Lausanne). The SA (Corana 1987) provides a strategy where a higher value of a function is acceptable under some conditions, not to be led to a local extremum. The PGSL is a global search technique based on the basic assumption that better points are more likely to be found in the neighbourhood of good points (Raphael 2000, Svanerudh 2002).

Therefore, this study first identifies optimum values using a MGA, which has a better searching ability than the simple genetic algorithm. To solve the convergence problem at later stage, we employed, hybrid algorithms that combine the global GA followed by local search algorithms (DFP or MGA). The hybrid algorithm using DFP method incorporates the advantages of both a genetic algorithm and gradient search technique. We call LZGA (Local Zooming GA) for the other hybrid algorithm of global GA and local GA at zoomed area. The enhancement of above hybrid algorithms is verified by investigating the gate optimum problem.

The installation of gates in dams is essential to regulate the flow-rate and to ensure the safety of dams. There are various types of gates with unique characteristics. Among these, the radial gate (Tainter gate) is widely used to regulate the flow-rate of huge dams due to its accuracy in regulating the flow-rate, easy opening and closing, endurance etc.

Yan (1991) studied the optimum design of dynamic characteristics radial gates using a sensitivity analysis and experimental modal analysis. Jiang (1994) researched the flow-induced vibrations of radial gates using the model examination method. Golliard (1998) improved the working capability of radial gates and their security using the concept of a fusegate. Anami (1998) analysed the vibration and damping characteristics of radial gates. However, although the selection of supporting points is very important in the design of a radial gate, there has been relatively little research on the optimum design of the location of radial arms. As such, the design of a radial gate generally depends on the experience of the designers. Therefore, this study focuses on the optimal design of the location of radial arms, then the results are compared with those of experience-based designs.

An attempt is made to demonstrate the usefulness and importance of optimization when selecting the location of a radial arm. Based on the above information, two types of radial gate are considered: 2-radial arm type and 3-radial arm type.

## 2. Genetic algorithm

GAs are stochastic global search methods that mimic the concept of natural evolution. Due to the nature of the algorithm, their successful application has been mostly restricted to optimization problems whose solution can be conveniently represented in binary form. However, there is a rising interest in applying genetic algorithms to continuous optimization problems, especially since there is no need for initial estimates, which is an important advantage over other stochastic search methods, such as simulated annealing. Therefore, in this paper GAs are applied for continuous variable optimization. A micro genetic algorithm (MGA) is briefly introduced and two hybrid algorithms are proposed to improve the local-tuning ability.

### 2.1 Micro genetic algorithm

Krisnakumar (1989) proposed a micro GA which has a good performance in the case of very small populations, whereas Carroll (1996) dealt with problems using other operators. De Jong (1975) showed that MGAs improved both the initial and later performance compared with simple genetic algorithms. MGAs converge faster to a near optimum design and can avoid premature convergence occurring in small population problems where the optimization procedure has to restart after populations are recomposed if they almost converge to one point to maintain a diversity of genetic information. The genetic operators used are as follows. The selection operators are the tournament selection and elitist strategy. The crossover operators are a one-point crossover, plus the crossover probability is  $P_c = 1$ , which means parent pairs crossover based on the need for earnest information exchange between individuals. MGAs introduce sufficient diversity every time, since an MGA restarts with new populations recomposed by optimum individuals in converged populations, and the remaining individuals are created arbitrarily if individuals converge close to any one point. Therefore,

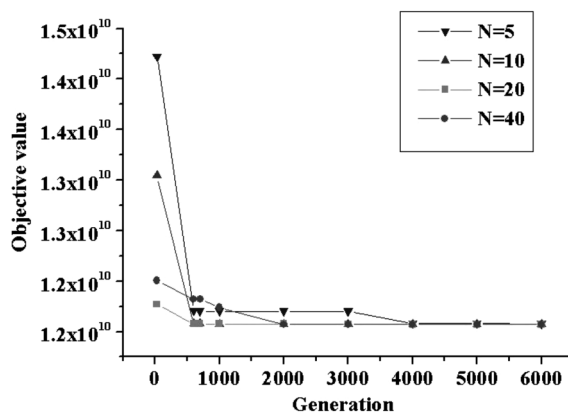


Fig. 1 Convergence in case A (2-design variables)

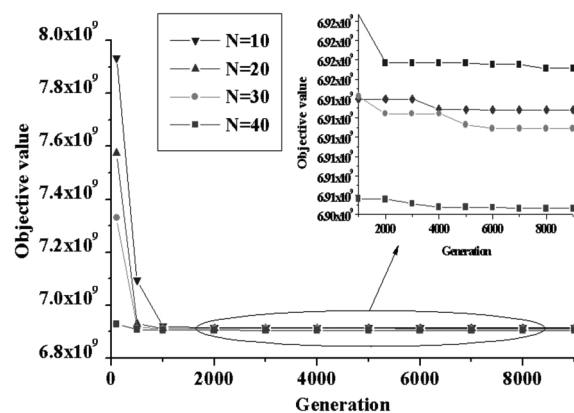


Fig. 2 Convergence in case B (3-design variables)

no additional mutation operators are needed. As such, the mutation probability fixed in  $P_m = 0$ .

Figs. 1 and 2 show the convergence processing of an object function with respect to generation evolution according to a change in the individual populations for case A and case B. In the case of A (two design variables) the object function became small after 700 generations for different population numbers. In the case of B (three design variables) the population number for an optimum performance increased compared to the case of two design variables. This was because the search region was magnified. Yet MGAs that can efficiently search small populations become less effective in the case of exceeding the population number for the optimum performance. Generally, because of poor local fine-tuning an MGA can not give a good solution accuracy and consumes much computing time. Accordingly, this paper presents a hybrid type GA to overcome this problem.

### 2.2 Hybrid algorithm I ; Combining MGA + DFP

This hybrid algorithm incorporates the advantages of both a genetic algorithm and gradient search techniques. A GA reaches a point closer to a global solution, then a gradient search algorithm searches for an accurate solution using this point as the initial point. As the local search algorithm, the DFP (Davidon-Fletcher-Powell) method is adopted from among the variable metric methods. When the change in the objective function becomes very small, this algorithm takes the generation as the initial point to reduce the computing time, for example, 700 generations in the case of A (2-design variables) and 4000 generations in the case of B (3-design variables). It is well known that the DFP method as a local search algorithm can converge to a local optimum value without preliminary knowledge. However the proposed hybrid algorithm converges to a global optimum value. Fig. 3 shows a flow chart of this algorithm.

### 2.3 Hybrid algorithm II ; Combining MGA + Local genetic algorithm

In this hybrid algorithm, a MGA is performed generation by generation until the objective function changes no more, then we have approximate optimum solution at  $Z_{MGA}$ . The gradients of

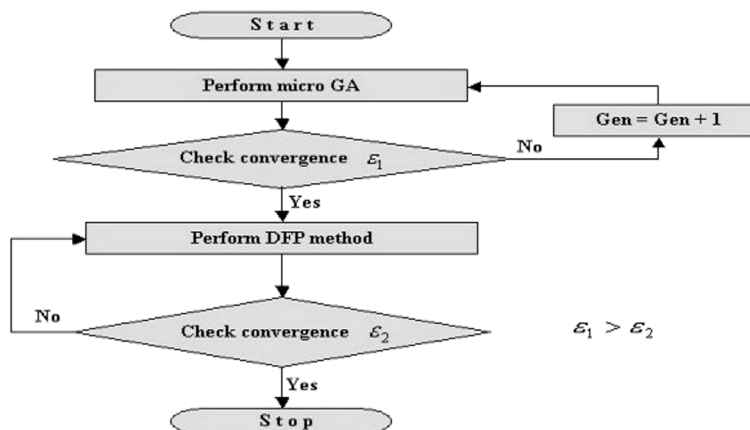


Fig. 3 Flow chart combining micro GA with DFP

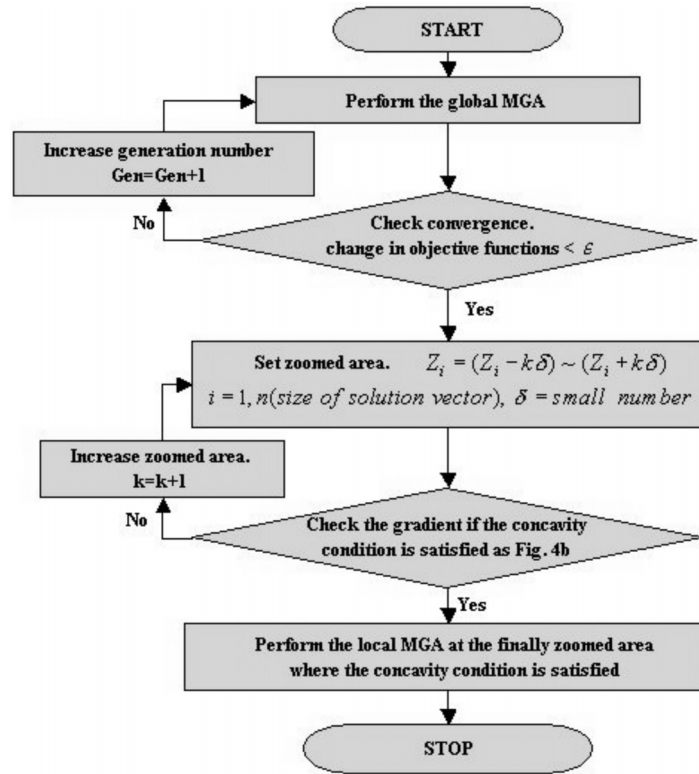


Fig. 4(a) Flow chart combining micro GA with local GA

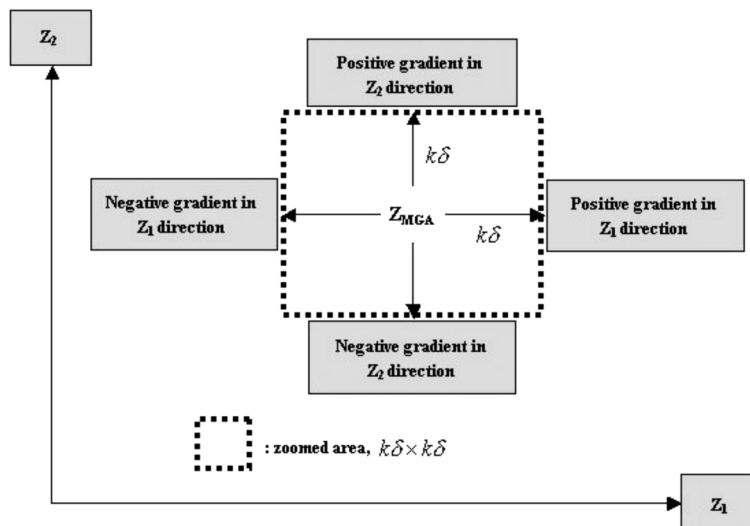


Fig. 4(b) Signs of gradients at concavity condition

Table 1 Optimum values by different optimum tools in the case A

Case A	Micro GA (N=10)	MGA+DFP	MGA+LGA
Convergence Generation	1000	700	700
Objection Function	0.115735E+11	0.115711E+11	0.115711E+11

Table 2 Optimum values by different optimum tools in the case B

Case B	Micro GA (N=10)	MGA+DFP	MGA+LGA
Convergence Generation	9000	4000	4000
Objection Function	0.690497E+10	0.690488E+10	0.690488E+10

the objective function along the design variables are checked, if the concavity condition (Himmelblau 1972) is satisfied at the boundary of small zoomed area (Fig. 4b). If the condition is not satisfied, the small zoomed area is increased by  $\delta$ . After many iterations we finally have the concavity conditions at the boundary of final zoomed area ( $k\delta \times k\delta$ ) centered at  $Z_{MGA}$ . With the elitist solution from the global GA (approximate optimum solution,  $Z_{MGA}$ ) and the concavity condition, we have the optimum point within the final zoomed area [ $Z_i = (Z_i - k\delta) \sim (Z_i + k\delta)$ ]. From this point we perform a local GA for the small finally zoomed area, which probably contains the optimum point. Usually, this area is very small compared with the original one, therefore we have tremendously increased convergence rate (remember that the first approximate solution prematurely converged to an inexact optimum point).

Tables 1 and 2 show the optimum values for above three algorithms. Clearly the hybrid algorithm produced a solution with a better accuracy than the Micro GA, plus reduced the computing time. When the results of the case A (2-design variables) and case B (3-design variables) are compared, the computing time of the case B was longer due to a wider searching region.

We can tell that the hybrid algorithms have the same optional solution (0.690488E+10), the original MGA still has no actual optimal solution (0.690497E+10) with over double size of generations than the others.

### 3. Structure of radial gate and governing equations

#### 3.1 Structure of radial gate

In radial gates, the part of the radial gate that resists water pressure and ice pressure related to the freezing of the water surface is called the skin plate. Fig. 5 shows the structure of a radial gate where the skin plate, supported by 2 arms, is resisting both ice pressure and hydro-static pressure.

In Fig. 5 ELH, ELS, and  $P_{ice}$  are the height of the water surface, height of the bottom of the skin plate, and ice pressure related to the freezing of the water surface in winter, respectively. B represents the width of the skin plate. To calculate the force of each arm supporting the skin plate, the dead weight of the skin plate has to be considered in addition to aforesaid  $P_{ice}$  and hydrostatic pressure, as shown in Fig. 5. In Fig. 5, the depth of the water,  $h$ , is ELH-ELS. The projected area of the skin plate is used to calculate the vertical and horizontal components of the resultant force

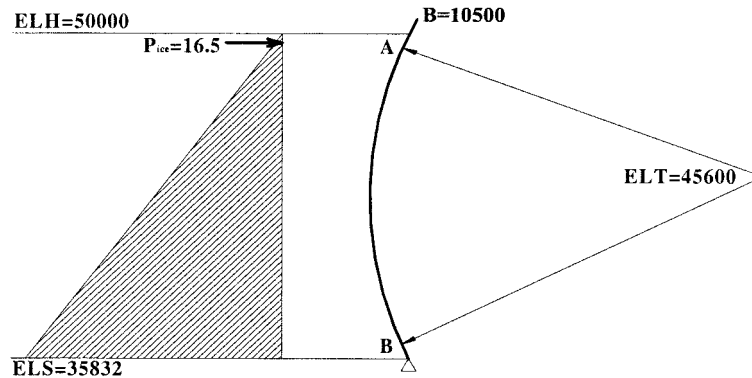


Fig. 5 Model of the radial gate with 2-arm

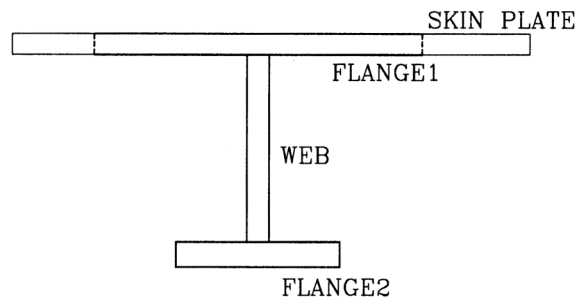


Fig. 6 Vertical girder

working on the skin plate due to hydrostatic pressure in proportion to the depth of the water. That is, the circular skin plate is assumed to be straight. Radial gates have vertical girders that support the load first. Fig. 6 shows an H-type vertical girder supporting the skin plate of a vertical girder. The vertical girder is connected to the horizontal girder and arms, and is designed to support the skin plate. As shown in Fig. 6, an H-type vertical girder is composed of a flange 1, flange 2, and web. The section modulae  $Z_1$  and  $Z_2$  are different from each other because the sizes of the upper and lower flange are different from each other. Radial gates can be divided into 2-arm and 3-arm types, according to the number of arms. Whereas the governing equation for a 2-arm type is statistically determinate, the governing equation for a 3-arm type is statistically indeterminate.

### 3.2 Governing equation of 2-arm type radial gate

Fig. 7 shows the water pressure on a skin plate of a radial gate supported by 2 arms. Although the vertical girder that supports the skin plate is curved, it can be treated as a straight beam when the ratio of the radius of the curvature to the thickness ( $R/t$ ) is over 20 (Ugural 1995). Here, it was treated as a straight beam because the  $R/t$  ratio was almost 80.

From the equilibrium equations  $\Sigma F = 0$ ,  $\Sigma M_A = 0$ , the reaction forces and reaction moments of points A and B become Eqs. (1) and (2) and Eqs. (3) and (4), respectively

$$R_B = \frac{\frac{1}{3}\gamma(L_2 + L_3)^2(h_3 - h_1) + \frac{1}{2}\gamma(L_2 + L_3)^2h_1 - P_{ice}L_4 - \frac{1}{6}\gamma L_1^2h_1 + P_s(L_2 + L_3)}{L_2} \quad (1)$$

$$R_A = P_{ice} + \frac{1}{2}\gamma L_A h_3 + P_s - R_B \quad (2)$$

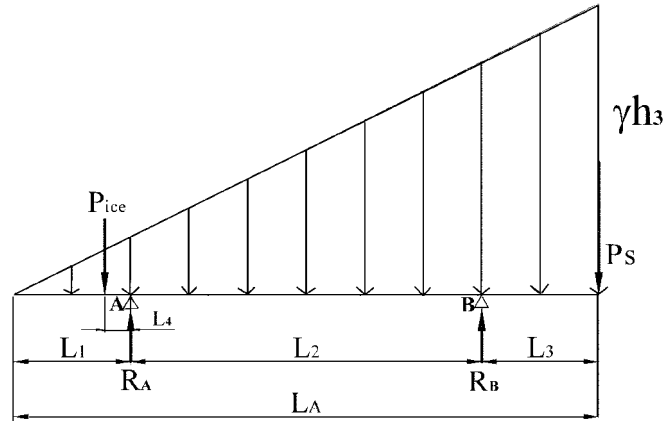
$$M_A = -P_{ice}L_4 - \frac{1}{6}\gamma L_1^2h_1 \quad (3)$$

$$M_B = -P_{ice}(L_4 + L_2) - \frac{1}{6}\gamma(L_1 + L_2)^2h_2 + R_A L_2 \quad (4)$$

The objective is to determine the location value of the maximum moment. When  $x$  is the distance from point A, as in Fig. 7, the moment of  $x$  is equal to Eq. (5)

$$M_{AB} = -\frac{1}{2}\gamma L_1 h_1 \left( \frac{L_1}{3} + x \right) - P_{ice}(L_4 + x) + R_A x - \frac{1}{2}\gamma x^2 h_1 - \frac{1}{6}\gamma \frac{(h_2 - h_1)}{L_2} x^3 \quad (5)$$

To identify the maximum, the derivative of  $M_{AB}$  with respect to  $x$  should equal 0. From here, the maximum moment  $M_{max}$ , can be obtained.



- $\gamma h$  : hydrostatic pressure
- $P_{ice}$  : ice load
- $P_s$  : horizontal component of the reaction at bottom of the skin plate

Fig. 7 Free body diagram of radial gate with 2 arms

$$M_{ABmax} = \frac{L_2 \left\{ -h_1 + \sqrt{h_1^2 + \frac{2(h_2 - h_1) \left( R_A - \frac{1}{2} \gamma L_1 h_1 - P_{ice} \right)}{\gamma L_2}} \right\}}{h_2 - h_1} \quad (6)$$

Here,  $h_1 = L_1$ ,  $h_2 = L_1 + L_2$ ,  $h_3 = L_1 + L_2 + L_3$

Thus, the maximum moment in a vertical girder is one of  $M_A$ ,  $M_B$  and  $M_{ABmax}$ , plus the section modulus of a vertical girder can be decided for this maximum moment.

### 3.3 Governing equation of 3-arm type radial gate

In the case of a 3-arm radial gate, the number of unknowns is three, whereas the number of equilibrium equations is two. That is, the problem is statistically indeterminate. Fig. 8 shows the free body diagram of a 3-arm type radial gate.

To solve the above statistically indeterminate problem, Fig. 8 is divided into Figs. 9(a) and 9(b).

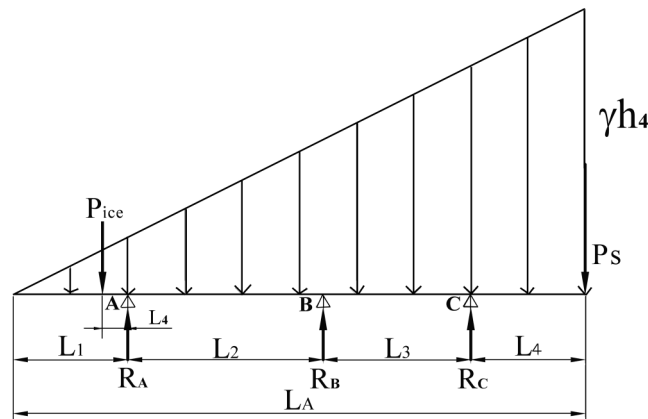


Fig. 8 Free body diagram of radial gate with 3 arms

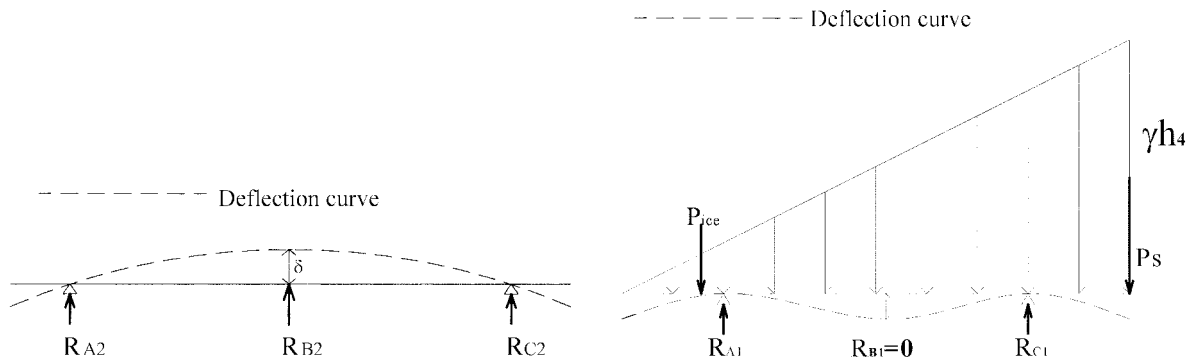


Fig. 9(a) Reaction curve diagram

Fig. 9(b) Deflection curve diagram

The solution of a statically indeterminate beam can be obtained using the singularity function method. First, when the load acts at the simple-supports-beam, as shown in Fig. 9(a), the deflection is as follows.

$$v_{B2} = \delta = \frac{R_{B2}L_3L_2}{6EI_z(L_2 + L_3)} \{(L_2 + L_3)^2 - L_2^2 - L_3^2\} \quad (7)$$

The deflection at point B can be calculated by applying the singularity method to the simple-supports-beam with the distributed load in Fig. 9(b). The singularity function applied is equal to Eq. (8).

$$q = -P_{ice} \langle x - (L_1 - L_5) \rangle_{-1} + R_{A1} \langle x - L_1 \rangle_{-1} + R_{C1} \langle x - (L_1 + L_2 + L_3) \rangle_{-1} - P_s \langle x - L_A \rangle_{-1} - \gamma \langle x \rangle^1 \quad (8)$$

When integrating the beam equation with Eq. (8), the deflection is as follows:

$$EI_z v = -\frac{P_{ice}}{6} \langle x - (L_1 - L_5) \rangle^3 + \frac{R_{A1}}{6} \langle x - L_1 \rangle^3 + \frac{R_{C1}}{6} \langle x - (L_1 + L_2 + L_3) \rangle^3 - \frac{P_s}{6} \langle x - L_A \rangle^3 - \frac{\gamma}{120} \langle x \rangle^5 + C_1 x + C_2 \quad (9)$$

in which  $E$  and  $I_z$  represent the modulus of elasticity and inertial moment, respectively. When applying the boundary condition that the deflection at points A and C is 0, the equations for the constants  $C_1$  and  $C_2$  are as follows:

Point A ( $x = L_1$ )

$$C_1 L_1 + C_2 = \frac{P_{ice}}{6} L_5^3 + \frac{\gamma}{120} L_1^5 \quad (10)$$

Point C ( $x = L_1 + L_2 + L_3$ )

$$C_1 (L_1 + L_2 + L_3) + C_2 = \frac{P_{ice}}{6} (L_2 + L_3 + L_5)^3 - \frac{R_{A1}}{6} (L_2 + L_3)^3 + \frac{\gamma}{120} (L_1 + L_2 + L_3)^5 \quad (11)$$

By substituting  $x = L_1 + L_2$  into Eq. (9), the deflection at point B can be obtained.

$$EI_z v_B = -\frac{P_{ice}}{6} (L_2 + L_5)^3 + \frac{R_{A1}}{6} (L_2)^3 - \frac{\gamma}{120} (L_1 + L_2)^5 + C_1 (L_1 + L_2) + C_2 \quad (12)$$

When substituting  $v_B$  into Eq. (7),  $R_{B2}$  can be obtained. The reaction forces  $R_{A2}$  and  $R_{C2}$  in Fig. 9(a) are as follows:

$$R_{A2} = -\frac{R_{B2}L_3}{(L_2 + L_3)} \quad (13)$$

$$R_{B2} = \frac{3(L_2 + L_3)}{(L_2 L_3)^2} \left[ -\frac{P_{ice}}{6}(L_2 + L_5)^3 + \frac{R_{A1} L_2^3}{6} - \frac{\gamma}{120}(L_1 + L_2)^5 + C_1(L_1 + L_2) + C_2 \right] \quad (14)$$

$$R_{C2} = -R_{A2} - R_{B2} \quad (15)$$

Using the relation between the force and the moment in Fig. 9(b),  $R_{A1}$  and  $R_{C1}$  become Eqs. (16) and (18), respectively.

$$R_{A1} = \frac{P_{ice}(L_2 + L_3 + L_5) + \frac{1}{6}\gamma h_3(L_1 + L_2 + L_3)^2 - P_s L_4}{(L_2 + L_3)} \quad (16)$$

$$R_{B1} = 0 \quad (17)$$

$$R_{C1} = P_{ice} - R_{A1} + \frac{1}{2}\gamma h_4 L_A + P_s \quad (18)$$

Using the above Eqs. (13)-(18), the reaction forces of arms A, B and C are as follows:

$$R_A = R_{A1} + R_{A2} \quad (19)$$

$$R_B = R_{B1} + R_{B2} \quad (20)$$

$$R_C = R_{C1} + R_{C2} \quad (21)$$

and the moments for each arm are as follows (Fig. 8):

$$M_A = -P_{ice} L_5 - \frac{\gamma}{6} h_1 L_1^2 \quad (22)$$

$$M_B = -P_{ice}(L_2 + L_5) + R_A L_2 - \frac{\gamma}{6} h_2 (L_1 + L_2)^2 \quad (23)$$

$$M_C = -P_{ice}(L_2 + L_3 + L_5) + R_A(L_2 + L_3) + R_B L_3 - \frac{\gamma}{6} h_3 (L_1 + L_2 + L_3)^2 \quad (24)$$

Here,  $h_1 = L_1$ ,  $h_2 = L_1 + L_2$ ,  $h_3 = L_1 + L_2 + L_3$

The maximum moment occurring in a vertical girder is one of the maximum bending moments:  $M_A$ ,  $M_B$ ,  $M_C$ , or  $M_{AC}$ . The magnitude of the maximum bending moment determines the section modulus of a vertical girder.

## 4. Weight minimization of radial gate

### 4.1 Formulation of optimum problems

Selecting the location of a radial arm is very important because the size of the member supporting the working stress is affected by the location of the radial arm. The weight can be obtained by the density times the volume calculated based on the size of the member. Therefore, the weight can be

minimized by an economic design that controls the location of 2-arm type or 3-arm type. In this study, weight minimization is obtained by minimizing the volumes because the density is constant. Therefore, the volume equations are as follows.

(CASE I) girder only

$$V_{\max} = \frac{N_1 \times M_{\max} \times L_g}{S_g \times f_1} \quad (25)$$

(CASE II) girder and non-equal arm cross-section

· 2-arm type

$$V_{\max} = \frac{N_1 \times M_{\max} \times L_g}{S_g \times f_1} + \frac{(R_a + R_b) \times L_a \times N_2}{S_a} \quad (26)$$

· 3-arm type

$$V_{\max} = \frac{N_1 \times M_{\max} \times L_g}{S_g \times f_1} + \frac{(R_a + R_b + R_c) \times L_a \times N_2}{S_a} \quad (27)$$

(CASE III) girder and equal arm cross-section

· 2-arm type

$$V_{\max} = \frac{N_1 \times M_{\max} \times L_g}{S_g \times f_1} + \frac{(R_{\max}) \times L_a \times N_2 \times 2}{S_a} \quad (28)$$

· 3-arm type

$$V_{\max} = \frac{N_1 \times M_{\max} \times L_g}{S_g \times f_1} + \frac{R_{\max} \times L_a \times N_2 \times 3}{S_a} \quad (29)$$

Where,  $N_1$  : Vertical girder number

$N_2$  : Arm number

$L_g$  : Vertical girder length

$L_a$  : Arm length

$S_g$  : Vertical girder allowable stress

$S_a$  : Arm allowable stress

$R_{\max}$  : Max. reaction of supporting point

$M_{\max}$  : Max. moment of vertical girder

$f_1$  : The ratio of the section modulus to section area =  $Z/A = 0.32h$  (Gere & Timoshenko 1995),

$h$  : Section height

CASE I only considers the girder. CASE II considers the girder and a non-equal arm (different arm sizes). CASE III considers the girder and an equal arm (identical arm sizes). Calculating the volumes based on the above equation satisfies the strength constraint condition. When optimizing the arm location on a radial gate, the independent variables are the length ratios, which are dimensionless with respect to the total length. The optimization problems can be formulated as follows:

Two-arm type

$$\begin{aligned}
 &\text{Minimize } f(\mathbf{R}) = \text{max. volume of gate} \\
 &\mathbf{R} = \{R_1 \ R_2 \ R_3\}^T \\
 &\text{subject to} \\
 &R_1 + R_2 + R_3 = 1 \\
 &R_i : \text{dimensionless lengths}
 \end{aligned} \tag{30}$$

Three-arm type

$$\begin{aligned}
 &\text{Minimize } f(\mathbf{R}) = \text{max. volume of gate} \\
 &\mathbf{R} = \{R_1 \ R_2 \ R_3 \ R_4\}^T \\
 &\text{subject to} \\
 &R_1 + R_2 + R_3 + R_4 = 1 \\
 &R_i : \text{dimensionless lengths}
 \end{aligned} \tag{31}$$

In the case of a 2-arm type, the value of  $R_3$  is decided automatically by  $R_1$  and  $R_2$  from the equation  $R_1 + R_2 + R_3 = 1$ . Therefore, the only independent variables used in optimization are  $R_1$  and  $R_2$ . A decrease in the section modulus satisfying allowable stress of a vertical girder under a given load condition can be obtained by comparing the values of the section modulus before and after optimization. As a result, the optimum weight according to the reduction in the section modulus can be obtained. In the case of a 3-arm type, the number of independent variables is three and the sum of the length ratios of each part must be one.

Table 3 shows the minimum section modulus and weight satisfying allowable stress in the case of a 2-arm type. Table 4 shows the minimum section modulus and weight satisfying allowable stress in the case of a 3-arm type.

In this study, the ratio of length before optimization was 0.5:1:0.5 in the case of a 2-arm, and 0.5:1:1:0.5 in the case of a 3-arm. Tables 3 and 4 show that the arm moments were equally

Table 3 Optimum results in the case of a 2-arm type

2-arm		Value before optimum	Optimum value		
			Girder Only	Girder and Non-equal Arm	Girder and Equal Arm
Ratio of length	$R_1$	0.25000	0.19381	0.19381	0.19380
	$R_2$	0.50000	0.67662	0.67662	0.67663
	$R_3$	0.25000	0.12957	0.12957	0.12957
Reaction (kg/mm)	$R_A$	0.37137E+2	0.52729E+2	0.52729E+2	0.52729E+2
	$R_B$	0.10493E+3	0.89341E+2	0.89341E+2	0.89341E+2
Moment (kg-mm/mm)	$M_A$	0.75006E+5	0.55255E+5	0.55255E+5	0.55253E+5
	$M_B$	0.15381E+6	0.55255E+5	0.55255E+5	0.55254E+5
Section modulus (mm <sup>3</sup> )	$Z_1$	0.77328E+7	0.27780E+7	0.27780E+7	0.27781E+7
	$Z_2$	0.64087E+7	0.23023E+7	0.23023E+7	0.23024E+7
Volume (mm <sup>3</sup> )	Girder Only	0.23905E+11	0.85877E+10	-	-
	Girder+Arm	0.26889E+11	-	0.11571E+11	0.12340E+11

Table 4 Optimum results in the case of a 3-arm type

3-arm		Value before optimum	Optimum value		
			Girder Only	Girder and Non-equal Arm	Girder and Equal Arm
Ratio of length	$R_1$	0.16667E+0	0.94167E-1	0.94167E-1	0.96218E-1
	$R_2$	0.33333E+0	0.46274E+0	0.46274E+0	0.49757E+0
	$R_3$	0.33333E+0	0.36789E+0	0.36789E+0	0.32980E+0
	$R_4$	0.16667E+0	0.75203E-1	0.75203E-1	0.76412E-1
Reaction (kg/mm)	$R_A$	0.40160E+2	0.30462E+2	0.30462E+2	0.32248E+2
	$R_B$	0.10903E+2	0.49199E+2	0.49199E+2	0.50179E+2
	$R_C$	0.91007E+2	0.62409E+2	0.62409E+2	0.59643E+2
Moment (kg-mm/mm)	$M_A$	0.46542E+5	0.25231E+5	0.25231E+5	0.25803E+5
	$M_B$	0.69769E+4	0.25231E+5	0.25231E+5	0.25801E+5
	$M_C$	0.81075E+5	0.25231E+5	0.25231E+5	0.25796E+5
Section modulus (mm <sup>3</sup> )	$Z_1$	0.40761E+7	0.12685E+7	0.12685E+7	0.12972E+7
	$Z_2$	0.33781E+7	0.10513E+7	0.10513E+7	0.10751E+7
Volume (mm <sup>3</sup> )	Girder Only	0.77921E+10	0.34524E+10	-	-
	Girder+Arm	0.15584E+11	-	0.69049E+10	0.77677E+10

distributed at supports in each arm in the case of the minimum weight radial gate except for the case of equal arm. This can be explained as follows. We made the sizes of cross-section of arms be equal for the convenience of manufacturing. That altered the optimal position of arms to result in unequal moments at the supports. The sum of the reaction force for each arm in the 2-arm and 3-arm types was always 0.14207E+3 kg/mm, thereby indicating indirectly that the governing equations in Sec 3.2 and 3.3 are correct. As depicted in Table 3, in the case of a 2-arm type, the section modulus of a vertical girder satisfying the safety constraints was only 36.0% after optimization. In addition, in Table 3, with weight optimization in the case of a 2-arm type, the weight was reduced by 64.0% compared to the value before optimization for CASE I, 56% for CASE II (different arm size), and 54% for CASE III (identical arm size).

In the case of a 3-arm type, the section modulus of a vertical girder satisfying the safety constraints was only 32% after optimization, as shown in Table 4. Furthermore, in Table 4, when optimization was accomplished in the case of a 3-arm type, the weight was reduced by 55% compared to the value before optimization for CASE I, 55% for CASE II (different arm size), and 50% for CASE III (identical arm size). As such, the optimum values for the length ratio, reaction, moment, and section modulus were the same for both CASE I and CASE II. The reason for this is that a vertical girder supports the load, which is then distributed to the arms. Meanwhile, in the case of different arm size (non-equal arms), the size of the arms are decided by the force at the respective supporting points. But, in the case of identical arm size, the optimized weight is larger than that in a non-equal arm case because shape of the arms is made identical to that of the arm supporting the largest force.

## 5. Conclusions

This study presented a structural analysis of a radial gate under a working load of water pressure and ice pressure for both 2-arm and 3-arm types. The weight of the radial gate was minimized using an optimization technique involving a genetic algorithm. A hybrid genetic algorithm was also applied to enhance the convergence speed and reduce the computing time. A summary of the results is listed as follows. First, for both the 2-arm and 3-arm cases of a radial gate, the relationship between the load and the bending moment was derived. Second, two hybrid algorithms were proposed to improve the local-tuning ability ; 1) GA + DFP incorporates the advantages of both a genetic algorithm and local search techniques. 2) GA + LGA used GA for global solution and LGA for local solution. These two algorithm were used to solve the convergence problems in a genetic algorithm. The last, in the design of a radial gate, the optimum problem is formulated that has to find the location of the arms for minimum volume ; 1) The weights of the optimized radial gates were appreciably lower than those of previously constructed gates. 2) The weight of a 2-arm type was heavier than that of a 3-arm type because the moment of a vertical girder in a 2-arm type is bigger than that of a 3-arm type. 3) A girder and equal arms were heavier than a girder and non-equal arms. This was due to non-optimal sizes of the cross-section of arms. However, A designer is more likely to select a girder and equal arms when considering the manufacture process, maintenance, dynamic behavior, etc.

## Acknowledgements

This work was supported by the Brain Korea 21 Project in 2003.

## References

- Anami, K. (1998), "In-water Streamwise Vibration of Folsom Dam 'Radial Gates' in California", *Flow-Induced Vibration and Transient Thermal-Hydraulics American Society of Mechanical Engineers, Pressure Vessels and Piping Division (Publication) PVP*, ASME, Fairfield, NJ, USA, **363**, 87-94.
- Arora, J.S. (1989), *Introduction to Optimum Design*, McGraw-Hill, Inc.
- Carroll, D.L. (1996), "Genetic algorithms and optimizing chemical oxygen-iodine lasers", *Developments in Theoretical and Applied Mechanics*, **18**, 411-424.
- Corana, A., Marchesi, M., Martini, C. and Ridella, S. (1987), "Minimizing multimodal functions of continuous variables with simulated annealing algorithm", *ACM Transactions on Mathematical Software*, **13**, 262-280.
- Gere, J.M. and Timoshenko, S.P. (1995), *Mechanics of Materials*, Third Edition, International Thosmon Publishing.
- Goldberg, D.E. (1989), *Genetic Algorithms in Search, Optimization, and Machine Learning*, Addison-Wesley, Reading.
- Golliard, D. (1998), "Innovative solution to a safety problem at Montsalvens Dam", *Int. J. Hydropower & Dams*, **5**(2), 63-65.
- Himmelblau, D.M. (1972), *Applied Nonlinear Programming*, McGraw-Hill.
- Hyundai Heavy Industries Co., Chungju Dam Data.
- Hyundai Heavy Industries Co., Hapchun Dam Data.
- Hyundai Heavy Industries Co., Yuncheon Dam Data.
- Jiang (1994), "Experimental study of radial gate vibration in spill way of Dongfeng arch dam hydraulic power

- station in Wu river”, *Journal of Dalian University of Technology*, **34**(1).
- De Jong, K.A. (1975), “An analysis of the behavior of a class of genetic adaptive systems”, Doctoral Dissertation, The University of Michigan, Ann Arbor, Michigan.
- Juvinall, R.C. (1991), *Fundamentals of Machine Component Design*, Second Edition, John Wiley & Sons, Inc.
- Krishnakumar, K. (1989), “Micro-genetic algorithms for stationary and non-stationary function optimization”, *SPIE, Intelligent Control and Adaptive Systems*, **1196**, 289-296.
- Kwon, Y.D., Kwon, S.B., Jin, S.B. and Kim, J.Y. (2003), “Convergence enhanced genetic algorithm with successive zooming method for solving continuous optimization problems”, *Comput. Struct.*, **81**, 1715-1725.
- Luenberger, D.G. (1973), *Introduction to Linear and Nonlinear Programming*, Addison-Wesley Publishing Company, Inc.
- Mitchell, M., Holland, J.H. and Forrest, S. (1993), “When will a genetic algorithm outperform hill climbing?”, *Advances in Neural Information Processing Systems*, J.D. Cohn, G. Tesauro and J. Alspector (Eds), Morgan Kaufmann, San Mateo, CA.
- Munson, B.R., Young, D.F. and Okiishi, T.H. (1990), *Fundamentals of Fluid Mechanics*, Second Edition, John Wiley & Sons, Inc.
- Raphel, B. and Smith, I.F.C. (2000), “A probabilistic search algorithm for finding optimally directed solutions”, *Proc. Construction Information Technology, Icelandic Building Research Institute, Reykjavic*, 708-721.
- Rao, S.S. (1996), *Engineering Optimization-Theory and Practice*, Third Edition, A Wiley-Interscience Publication.
- Seely, F.B. and Smith, J.O. (1952), *Advanced Mechanics of Materials*, Second Edition, John Wiley & Sons, Inc.
- Schraudolph, N.N. and Belew, R.K. (1992), “Dynamic parameter encoding for genetic algorithms”, *J. Mach Learn*, **9**, 9-21.
- Svanerudh, P., Raphael, B. and Smith, I.F.C. (2002), “Lowering costs of timber shear-wall design using global search”, *Engineering with Computers*, **18**, 93-108.
- Ugural, A.C. (1995), *Advanced Strength and Applied Elasticity*, Third Edition, Prentice-Hall, Inc.
- Yan, S.W. (1991), “Dynamic characteristic optimization Tainter gates and their optimization”, *J. Struct. Eng.*, **117**, 3261-3273.